Journal of Membrane Science 550 (2018) 91–100

Contents lists available at ScienceDirect

Journal of Membrane Science

journal homepage: www.elsevier.com/locate/memsci

Biocatalytic membranes prepared by inkjet printing functionalized yeast cells onto microfiltration substrates

Yingying Chen[a,1], Peng Gao[b,1], Mark J. Summe[b], William A. Phillip[b,*], Na Wei[a,*]

[a] Department of Civil & Environmental Engineering & Earth Sciences, University of Notre Dame, Notre Dame, IN 46556, United States
[b] Department of Chemical and Biomolecular Engineering, University of Notre Dame, Notre Dame, IN 46556, United States

ARTICLE INFO

Keywords:
Biocatalytic membranes
Surface displayed laccase
Inkjet printing
Bisphenol A
Acetaminophen

ABSTRACT

Biocatalytic cells displaying functional enzymes on their surface have the ability to catalyze the degradation of persistent micropollutants with high enzyme accessibility and stability. However, the high migration and limited processing capability of suspended biocatalytic cells remain major challenges for practical applications in water treatment. In this study, we fabricated biocatalytic membranes (BCMs) by immobilizing biocatalytic cells, i.e., Baker's yeast with cell surface display laccase (SDL), on microporous membranes via inkjet printing and chemical crosslinking. The incorporation of SDL biocatalytic cells on the surface of the membranes was confirmed by microscopy, elemental analysis, and enzyme assay tests. Moreover, it was demonstrated that the number of SDL cells incorporated and therefore, the enzyme activity of the BCMs, could be systematically controlled by altering the printing parameters. The viability, regeneration, and high storage stability of SDL cells were maintained in the BCM platform. Furthermore, the BCMs could be reused with high stability as they retained 76% of their initial activity after ten repeated reaction cycles. In comparison, the activity of freely-suspended SDL cells declined to 42% of their initial activity after ten reaction cycles. Finally, the effectiveness of BCMs in treating emerging contaminants was confirmed using bisphenol A and acetaminophen as substrates in proof-of-concept experiments. The results of this study establish that BCMs can address concerns related to the utilization of suspended biocatalytic cells by fixing them on a microporous substrate. With further study and optimization, BCMs have the potential to be incorporated into membrane-based separation and pollutant degradation processes.

1. Introduction

Emerging contaminants, such as unmetabolized pharmaceuticals, ingredients of personal care products, and endocrine-disrupting compounds, are persistent pollutants that are biologically active and potentially toxic to human health and the natural environment [1,2]. These contaminants are often referred to as micropollutants because their harmful effects can manifest at trace concentrations. Enzyme biocatalysis, which uses natural or engineered enzymes to speed useful chemical reactions, offers a potentially sustainable and environmentally-benign route to catalyze the degradation of micropollutants. Due to its advantages, including high activity, low energy requirements, low toxicity, and simple process control and maintenance [3–5], enzyme biocatalysis has received considerable attention recently. Prior studies have demonstrated the efficacy of enzyme biocatalysts in the degradation of emerging contaminants [6], such as bisphenol A (BPA) [7,8] estrogen [9,10], atrazine [11] sulfamethoxazole [12] and perchlorate [13,14]. To date, studies of biocatalytic enzymes have largely explored whole-cell and free enzyme systems. In whole-cell biocatalysts, enzymes require cell growth to be functional [15,16] and the substrates must be transported through the cell envelope to the active enzymes [15,17]. In contrast, free enzymes, which have been recovered from lysed cells, can be used as additives to allow the direct contact of enzyme and substrate in solution, which can lead to degradation kinetics that are 1–2 orders of magnitude more rapid than those observed in comparable whole-cell systems [17]. However, free enzyme systems face challenges of their own including short enzyme lifetimes, laborious purification and recovery processes, and the high costs associated with a single use of the biocatalytic material [18].

A novel category of biocatalysts has emerged with the advancement of cell surface display technology that could address the challenges of existing enzyme systems. With surface display technology, functional enzymes are expressed and displayed on the outer surface of microbial host cells by fusion with the cell wall or plasma membrane [19]. As

* Corresponding authors.
E-mail addresses: wphillip@nd.edu (W.A. Phillip), nwei@nd.edu (N. Wei).
[1] These authors have contributed equally.

https://doi.org/10.1016/j.memsci.2017.12.045
Received 31 October 2017; Received in revised form 15 December 2017; Accepted 16 December 2017
Available online 20 December 2017
0376-7388/

such, surface displayed enzymes are readily accessible to the substrate while the metabolic potential of enzyme synthesis in the cells is retained. Surface display of a diverse range of functional enzymes with potential applications in sensing, biofuel production, drug screening, and metal ion adsorption have been reported [20]. However, the application of cell surface displayed enzymes in micropollutant degradation is underexplored. Recently, we developed a surface displayed laccase (SDL) biocatalyst where fungal laccase was expressed on the surface of yeast cells [21]. Fungal laccase was initially identified as a lignin-modifying enzyme [22] and was subsequently found to be capable of catalyzing the oxidation of various recalcitrant organic compounds [23]. Our SDL biocatalyst retained the ability to degrade persistent organic micropollutants and it demonstrated enhanced stability compared to free laccase. Furthermore, the SDL cell could be easily prepared and regenerated through cell cultivation [21].

The successful transition of the promising SDL biocatalyst from the laboratory to industrial scales requires that several technological concerns are addressed. For example, bioreactors require the minimization of cell washout in order to maintain high concentrations of the biocatalysts and prevent the potential ecological risks associated with the release of genetically engineered cells [24]. Immobilization of enzymatically-active materials (e.g. free enzymes or whole cells) on microporous substrates is one method to limit the migration of biocatalysts because it constrains the enzymes or whole cells to the substrate structure [25]. In addition to helping prevent washout, sequestering the enzymatically-active material on a substrate could yield better stability as the substrate structure protects the enzymes or cells from the surrounding environment [26]. Furthermore, the recovery of enzymatically-active materials that are fixed to a solid substrate is easier compared to suspended materials, which simplifies the process of recovering and recycling the biocatalytic materials [27].

Microporous membranes are a commonly studied class of substrates for the immobilization of biocatalysts due to the abundance of membrane materials, pore structures, and functionalities that are available for use [28]. Additionally, the modified membranes can be readily integrated into membrane-based processes, e.g., biocatalytic reactors [29], dialysis systems [30], and sequential reaction-separation schemes where the membrane is used both as the solid substrate for enzyme immobilization as well as a separation device that permits the selective removal of the product from the reaction mixture [31]. While the enzymatically active material can be sequestered on the membrane surface by physical adsorption, chemical crosslinking provides a more stable linkage between the active material and the membrane [28]. Many efforts have investigated the immobilization procedures but little focus has been dedicated to how the enzymatically-active material is deposited onto the microporous substrate. In most cases, biocatalysts are loaded onto the microporous membranes by immersion of the membrane into a solution containing the biocatalyst or by filtration of suspended cells through the membrane [32]. However, these methods can be problematic when the available volume of the biocatalyst-containing solution is small and because they provide minimal control over the biocatalyst loading.

Inkjet printing is a well-known method for the high-throughput deposition of liquid materials at predefined locations that could potentially be used to immobilize biological agents on membrane substrates in a straightforward and systematic manner [33]. The capability of inkjet printing to deposit droplets of picoliter volumes with micrometer-length accuracy has been shown to be useful in the layer-by-layer deposition of films [34,35] and surface patterning of substrates [36–39] using a number of relevant materials [40–48]. For example, inkjet printing has been explored in regenerative medicine to generate tissues by printing primary cells into 3-dimensional (3D) scaffolds [42,46]. Cells containing recognition elements such as enzymes and reporter genes have been inkjet printed to fabricate sensing arrays [49,50]. The deposition of microbes onto nitrocellulose membranes was used in a report aimed at studying the growth of cells. In that case, the microporous membrane allowed for the delivery of nutrients to the cells [48]. However, inkjet printing of biocatalytic cells onto microporous membranes used in the environmental arena has not been reported.

In this study, we demonstrate a method to fabricate biocatalytic membranes (BCMs) through the deposition of SDL cells on a microporous membrane using an inkjet printing device. Using polymer composite inks prepared with SDL cells and polyvinyl alcohol (PVA) dissolved in deionized water, we demonstrate that the biocatalyst load and distribution on microfiltration membranes could be well controlled by inkjet printing. In turn, this capability allowed the enzyme activity of the BCMs to be systematically altered through modifications to the ink formulations and printing procedure. The BCMs streamlined the enzyme recycling process and demonstrated improved reusability compared with suspended SDL cells while maintaining a competitive bioactivity and ability to degrade emerging contaminants, such as bisphenol A and acetaminophen. This study reports the development of biocatalytic membranes by immobilizing yeast cells displaying enzymatically-active laccase as an effective alternative for treating persistent organic pollutants in water. The technique serves as a platform for fabricating biocatalytic membranes functionalized with yeast cells with surface displayed enzymes that have potential applications in pollutant degradations as well as other applications where the facile reuse of cells engineered with surface-displayed enzymes is needed.

2. Experimental

2.1. Materials, strains, and medium

Bisphenol A (BPA, ≥ 99%), Acetaminophen (APAP, ≥ 99%), D-glucose, D-(+)-galactose, 2,2-azinobis-3-ethylbenzothiazoline-6-sulfonate (ABTS, 99%), poly(vinyl alcohol) (PVA) powder (molecular weight: 89–98 kDa, 99+% hydrolyzed), and 25% (by weight) glutaraldehyde were purchased from Sigma-Aldrich (St. Louis, MO). Asymmetric super micron polysulfone microporous membranes with a thickness of 165–200 μm were purchased from Pall Corporation. The manufacturer reported a nominal pore size of 800 nm for the selective layer of the membrane and pores 50 times larger (~ 40 μm) at the opposite side of the asymmetric structure. We hypothesized that the large pores would allow the yeast cells (~ 5 μm) to penetrate into the membrane while the small pore size would restrict their passage out of the membrane. Moreover, this membrane was chosen as a substrate because it was easily wet with aqueous solutions, which is a critical feature for the deposition of the polymer composite inks. Restriction enzymes, ligase, and molecular reagents for polymerase chain reaction (PCR) were obtained from New England Biolabs (Beverly, MA). Primers for sequencing were synthesized by Integrated DNA Technologies (Coralville, IA). All other general chemicals and medium components were supplied by Fisher Scientific (Pittsburgh, PA). Deionized water (DI water) for all experiments was obtained from a Millipore water purification system.

The *Saccharomyces cerevisiae* strain EBY100 (MATa *ura* 3–52 *trp* 1 *leu*2Δ1 *his*3Δ200 *pep*4:*HIS3 prb*1Δ1.6 R *can*1 *GAL*) was obtained from ATCC® (Manassas, VA) and was used as the host cell for enzyme display. *Escherichia coli* TOP10 strain was used for gene cloning and manipulation. *E. coli* was regularly grown in Luria-Bertani medium at 37 °C and 100 μg mL^{-1} of ampicillin was added to the medium when required. The wild type EBY100 strain was regularly cultivated at 30 °C in yeast extract peptone dextrose (YPD) medium (10 g L^{-1} of yeast extract, 20 g L^{-1} of peptone and 20 g L^{-1} D-glucose).

2.2. Construction of surface display laccase (SDL) biocatalytic cells

The surface display laccase (SDL) biocatalytic cells were developed as described previously [21]. Briefly, the codon optimized *LAC3* from *T. versicolor* was synthetized by Genscript (Piscataway, NJ). The *LAC3* gene fragment was ligated into the pCTcon2 plasmid (Addgene, Cambridge, MA), yielding the plasmid pCTcon2-Lac3. *E. coli* TOP10 strain

Table 1
Plasmids and strains used in this study.

Plasmids, strains and membranes	Description	References
Plasmids		
pCTcon2	A yeast expression vector for protein surface display	[52]
pCTcon2-Lac3	*LAC3* expressed in pCTcon2	[21]
Strains		
EBY100	MATa *ura* 3–52 *trp* 1 *leu*2Δ1 *his*3Δ200 *pep*4:*HIS3* *prb*1Δ1.6R *can*1 *GAL*	[52]
SDL	EBY100 strain harboring pCTcon2-Lac3	[21]
control cell	EBY100 strain harboring pCTcon2	[21]

was used for plasmid cloning. The plasmid pCTcon2-Lac3 was transformed to the *S. cerevisiae* strain EBY100 to obtain SDL biocatalyst cells by using the LiAc/PEG method [51]. The control plasmid pCTcon2 (without *LAC3* gene) was transformed to EBY100 to obtain the control cell without surface displayed laccase. The constructed plasmids and strains in this study are listed in Table 1.

2.3. Cultivation and preparation of the SDL biocatalytic cells

The SDL biocatalytic cells and control cells were cultured to early stationary growth phase in synthetic complete medium without tryptophan (SC-trp medium) that contained 20 g L^{-1} glucose. Cell number quantified by optical density at 600 nm (OD_{600}) was measured by using an UV–visible light spectrophotometer (VWR International LLC, Radnor, PA). Cells were harvested by centrifugation and transferred into new SC-trp medium containing 20 g L^{-1} galactose, 2 g L^{-1} glucose and 0.1 mM $CuSO_4$ for protein expression induction by cultivating at 30 °C and 250 rpm for 18 h (OD_{600} ~ 3 to 4). The induced cells were harvested by centrifugation and washed twice with 0.1 M acetate buffer (pH = 5). The induced cells were suspended in acetate buffer to appropriate density and used as a homogenous source for preparing polymer composite ink or biocatalytic experiments.

2.4. Preparation of inks containing SDL cells and polyvinyl alcohol

Aqueous solutions that contained 1% (by weight) PVA were prepared and filtered through an Acrodisc 25 mm syringe filter fitted with a 1 μm glass fiber membrane. 4 mL of yeast cell solutions containing 4 × 10^6 cells mL^{-1}, 4 × 10^7 cells mL^{-1}, 4 × 10^8 cells mL^{-1} and 4 × 10^9 cells mL^{-1} were mixed with 4 mL of the 1% (by weight) PVA solution to prepare the composite inks.

2.5. Fabrication of biocatalytic membranes (BCMs)

The composite inks containing PVA and yeast cells were printed using a Jetlab 4A drop-on-demand inkjet printing system (Fig. S1). The spacing between ejected droplets of ink, the printing speed, and the droplet geometry were adjusted to obtain uniform coverage of the composite ink over the surface of the microporous substrate. Typical values for these parameters were in the range of 80 μm, 48 mm s^{-1}, and 65–85 μm, respectively. The ink solutions were deposited over a 1.9 cm × 1.9 cm area of the membrane surface that contained larger-pore sizes while vacuum (~ 10 psig) was pulled on the selective layer side of the membrane. Vacuum was applied throughout the whole duration of the printing process. The number of printed layers was controlled between 10 and 40 using a pre-programmed script. The membrane was dried in air. Then, the PVA was crosslinked by exposing the BCM to the vapor in the head space of a chamber filled with a 25% (by volume) glutaraldehyde in water solution. Unless otherwise noted, crosslinking was conducted at 45 °C for 40 min. Subsequently, the membrane was rinsed, immersed in water for 1 h, and then dried in air.

2.6. Scanning electron microscopy of BCMs

The BCMs were imaged using a FEI-Magellan 400 field-emission scanning electron microscope. After crosslinking the PVA, the yeast cells on the membrane surface were dehydrated by exposure to serial alcohol solutions (25%, 50%, 75%, 90%, 95%, 100% (by volume)). The membranes were subsequently dried in air [54]. The BCMs were sputter coated with 2 nm of iridium to prevent sample charging during imaging. An accelerating voltage of 5 keV and 13 pA were used to generate all SEM micrographs. Elemental maps of the membrane surface were obtained using an energy dispersive X-ray spectrometer (Bruker); an accelerating voltage of 10 keV and current of 1.6 nA were used.

2.7. Cell viability staining and fluorescence microscope imaging

To evaluate the viability of cells deposited onto the membrane, a 1 cm^2 section of biocatalytic membrane was washed twice in a buffer solution containing 10 mM Na-HEPES with 2% D-glucose. Staining of the membranes was then performed using the LIVE/DEAD® Yeast Viability kit (Invitrogen, USA) according to the manufacturer's protocol. The membrane was visualized using an EVOS FL fluorescence microscope. The green fluorescence signal from live cells was detected through a GFP light cube. Images were analyzed with the ImageJ software.

2.8. Laccase enzyme activity assays

The enzyme activity of the SDL biocatalytic cells and the BCMs were determined by measuring the oxidation rate of 2,2-azinobis-3-ethylbenzothiazoline-6-sulfonate (ABTS, a model substrate for laccase) [55]. Batch reactions were set up by suspending 0.2 cm^2 of the BCM or 4 × 10^5 of the SDL cells in a 1 mL mixture that consisted of 140 μL of 5.0 mM ABTS and 860 μL of 0.1 M acetate buffer (pH = 5, optimal pH for laccase activity [56]). The oxidation of ABTS was monitored using a colorimetric method. Specifically, the absorbance at 420 nm was measured as a function of time using an UV–visible light spectrophotometer (VWR International LLC, Radnor, PA) under continuous stirring. The catalytic oxidation rate of ABTS by laccase could be calculated from the change of the absorbance over time. This rate is quantified using units of enzyme activity (U), where one unit of enzyme activity is defined as the amount of enzyme required to catalyze 1 μmol substrate per minute [57]. All measurements were conducted in triplicate.

2.9. Bisphenol A (BPA) and acetaminophen (APAP) Degradation Experiments

The BPA and APAP degradation experiments were performed using BCM samples with an area of 2.25 cm^2 or SDL yeast cells at a concentration of 4 × 10^5 cells mL^{-1}. Both values corresponded to an enzyme activity of 0.4 mU mL^{-1} of the micropollutant-containing solution. These materials were added to 5 mL solution containing 1 μM BPA or APAP and 0.1 M sodium acetate buffer (pH = 5) in Erlenmeyer flasks. 1 μM ABTS was added to accelerate the reaction if needed. The flasks were incubated at 30 °C and 250 rpm. Aliquots of the supernatant liquid were taken periodically and their concentrations were measured. Reactions with bare membranes and membranes with control cells (i.e., those that did not display laccase on their surface) were set up as the abiotic control and the negative biological control, respectively. Experiments were conducted in triplicate. The concentration of BPA and APAP was quantified using a high performance liquid chromatograph (Waters 2690 series) equipped with a photodiode array detector under the wavelength of 230 nm and with an Eclipse XDB-C18 column (Agilent Technologies, Santa Clara, CA). The column was eluted with methanol and water solution (v/v = 60:40) under the flow rate of 1 mL min^{-1} at 25 °C.

An actual wastewater sample was collected from the outlet of the secondary clarifier of the municipal wastewater treatment plant in

South Bend, IN. The water sample was filtered (0.45 μm) and then stored at 4 °C until use. The water was analyzed according to standard methods [58] and the characteristics are described in our previous publication [21].

2.10. Hydraulic permeability measurements of BCMs

The procedure for measuring the hydraulic permeability of a membrane was described in previous work [36,53]. Briefly, the BCM was mounted in a dead-end stirred cell (model 8003, Amicon) and the reservoir above the BCM was filled with DI water. A range of pressures from 0 to 5 psi was applied to the feed side of the membrane using nitrogen gas. The water that permeated through the membrane was collected in a scintillation vial that rested on a balance. The mass of the water that permeated into the vial was recorded periodically using a computer running Labview software (National Instruments). The mass vs. time data was used to calculate the hydraulic permeability of the BCMs.

3. Results and discussion

3.1. Fabrication of biocatalytic membranes using inkjet printing devices

The preparation of BCMs involved the formulation of a polymer composite ink; deposition of the ink onto a membrane substrate; and crosslinking of the polymer matrix to fix the cells to the membrane. The designs of the ink formulation, the printing protocol, and the PVA crosslinking conditions were all factors that influenced the successful deposition and attachment of enzymatically-active yeast cells to the microporous membrane supports. As such, specific details regarding experimental results that informed the choice of these conditions are discussed below.

3.1.1. Formulation and deposition of composite inks

The polymer composite inks were formulated with PVA as the matrix material due to the biocompatibility, solubility in water, and simple crosslinking protocols of PVA [59]. The concentrations of SDL cells in the composite inks were carefully chosen because the cells were comparable in size to the 50-μm-diameter of the printhead orifice. This lead to sieving effects that reduced the concentration of cells in ejected droplets relative to the parent ink solution (Table 2). Yet, the highest concentration of cells used in this study, 2×10^9 cells mL^{-1}, did not clog of the orifice of the printhead or significantly reduce the enzymatic activity of cells that passed through the printhead. In particular, after accounting for the reduced concentration of SDL cells in the ejected droplets, a comparison of the enzymatic activity of the ejected droplets and the parent composite inks demonstrated a small, 2–5%, reduction in enzymatic activity upon printing.

3.1.2. Immobilization of SDL cells on membranes by crosslinking

After deposition of the ink on the microporous membrane, the PVA matrix needs to be crosslinked to secure the SDL cells to the membrane, which helps prevent leakage of the biocatalyst into solution. Crosslinking PVA for extended lengths of time at high temperatures promotes higher crosslinking densities. However, the crosslinking agent utilized in this study, glutaraldehyde, is a disinfectant that can harm cell viability and enzyme activity. Fig. S2 shows how different crosslinking durations affected the enzyme activity and fixation of cells to the BCMs. A crosslinking duration of 40 min at 45 °C was implemented because it was found to effectively balance the need to affix the cells to the microporous membrane while preserving the cell viability and enzyme activity. A detailed discussion regarding the data that guided this choice is available in the Supplemental information. We quantified the enzyme activities of biocatalytic membranes immediately after printing (without rinsing in water for 2 h) and after crosslinking. It was found that crosslinking for 40 min led to a 45.7% enzyme inactivation. Additionally, we compared the enzyme activities of the same amount of cells printed on the membranes to those suspended in the ejected droplets. There was a 26.5% of decrease of the enzymatic activity after printing, which might be due to the inaccessibility of some cells after deposition on the membranes.

The activities of four samples obtained from different sections of the same BCM coupon were measured to examine the distribution of cells over the BCM. Table S1 shows the results of these measurements, which demonstrate that the activities of the four samples were all within 20% of each other, indicating a relatively uniform coverage of SDL cells. This was corroborated by fluorescent imaging of the cells on the membrane. Specifically, we accessed the viability of the immobilized SDL cells after the inkjet printing and crosslinking processes. A 1 cm^2 BCM-2.0-X was stained using a Live/Dead Yeast Viability Kit (Invitrogen) and then imaged using fluorescent microscopy. The stained cells, which were alive, appeared green as shown in Fig. 1**a**. The high number of green cells are dispersed evenly across the micrograph indicating the ability of the process to deposit the yeast cells uniformly.

Scanning electron microscopy analysis was also used to visualize the SDL cells immobilized on the BCMs. A top-view micrograph of a BCM is shown in Fig. 1**b**. In this micrograph, a false red color was applied to the SDL cells for simple identification. Energy-dispersive X-ray spectroscopy analysis was performed to make the assignment of cells on the surface. For example, a high magnification micrograph and corresponding elemental maps of phosphate and sulfur for a single cell clearly distinguished between the phosphate-rich cell and the sulfur-rich polymeric membrane (Fig. 2). Taken together these micrographs demonstrate the ability of the inkjet printing process to deposit SDL cells on all printed regions of the BCMs.

3.2. Effects of deposition conditions on enzymatic activity of the BCMs

Enzymatic activity is critical to the evaluation of BCM performance. Inkjet printing provided a method to control these parameters through systematic alterations of the cell concentration in the polymer composite inks and the number of layers of ink printed onto the membrane. The effects of these conditions on the enzymatic activity of the BCMs are shown in Fig. 3. A higher initial concentration of cells led to higher activity, which can be observed by comparing the data sets for the 2×10^8 cells mL^{-1} and 2×10^9 cells mL^{-1} ink formulations. This is consistent with the results presented in Table 2, which demonstrated that a higher initial concentration of cells resulted in a higher concentration of cells ejected through the printhead onto the membrane surface. The number of printed layers also impacted the enzyme activity of the BCMs

Table 2
Comparison of cell concentration and enzyme activity in the polymer composite ink and cell concentration in the ejected droplets.

Cell concentration in composite ink (cells mL^{-1})	2.0×10^6	2.0×10^7	2.0×10^8	2.0×10^9
Enzyme activity of composite ink (mU mL^{-1} $OD_{600}{}^{-1}$)	3.77	4.00	4.00	3.72
Cell concentration in the ejected droplets (cells mL^{-1})	9.6×10^5	4.7×10^6	3.4×10^7	2.7×10^8
Enzyme activity of the ejected droplets (mU mL^{-1} $OD_{600}{}^{-1}$)	3.65	3.81	3.76	3.62
Percentage of cells ejected through printhead (%)	47.7	23.6	16.9	13.5
Enzyme activity in the ejected droplets relative to enzyme activity in composite ink (%)	96.7	95.3	95.0	98.0

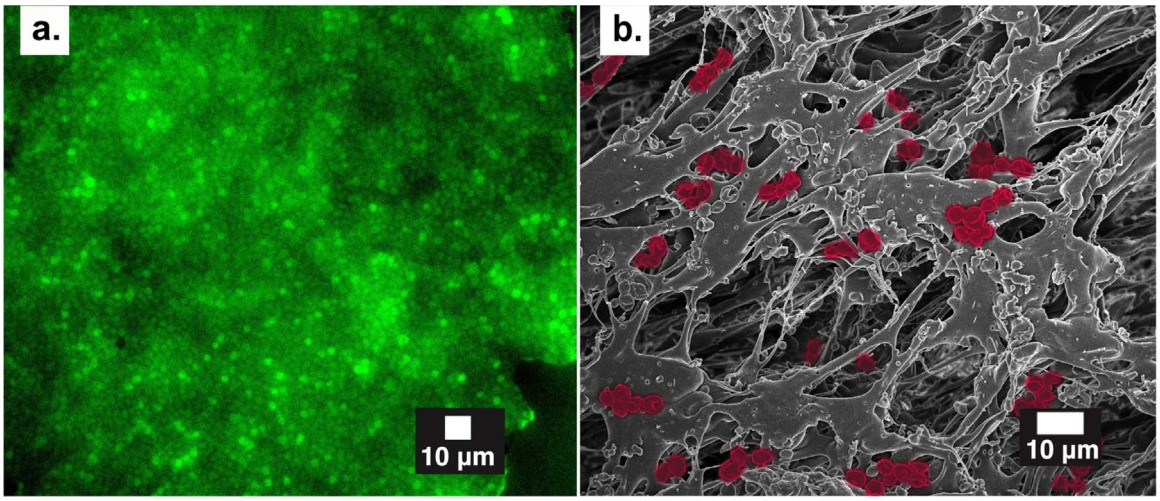

Fig. 1. Fluorescent micrograph (a) and a top-view SEM (b) of a biocatalytic membrane (BCM). Thirty layers of an ink based on a 0.5% (by weight) poly(vinyl alcohol) in DI water solution containing 2×10^9 yeast cells per mL were deposited onto an asymmetric polysulfone (PSf) membrane to generate the BCM. Following deposition, the yeast cells were fixed to the BCM using the vapor above a 25% (by volume) glutaraldehyde solution. Yeast cells have a characteristic size of ~ 5 μm. In the fluorescent micrograph, cells stained green by a live-dead staining assay are live cells. In the SEM micrograph, a false red color was applied to the SDL cells for simple identification. (For interpretation of the references to color in this figure legend, the reader is referred to the web version of this article.)

with the enzymatic activity increasing with the number of printed layers for both the BCMs prepared with 2×10^8 cells mL^{-1} and 2×10^9 cells mL^{-1} ink formulations (Fig. 3).

Over the range of conditions studied, inkjet printing allowed the enzymatic activity of the BCMs to be controlled in a systematic manner. Specifically, the linear increase in enzyme activity with number of printed layers could be estimated by starting with the enzymatic activity of the parent ink and accounting for the reductions in activity that resulted from sieving by the printhead, crosslinking, and cell inaccessibility. Further details regarding this calculation are available in the Supplemental information. In addition to guiding the fabrication of the BCMs utilized in this study, this knowledge provides targeted areas of improvement for the further development of BCMs that exhibit higher enzymatic activities. For example, it is likely that higher cell concentration, milder crosslinking conditions, and/or a greater number of printed layers are future avenues of research to be considered. Thirty printed layers was chosen for the rest of the study to minimize cell sedimentation in the ink reservoir, which increases as the printing duration prolongs [42]. A reservoir that continually stirred the ink could help optimize this design choice.

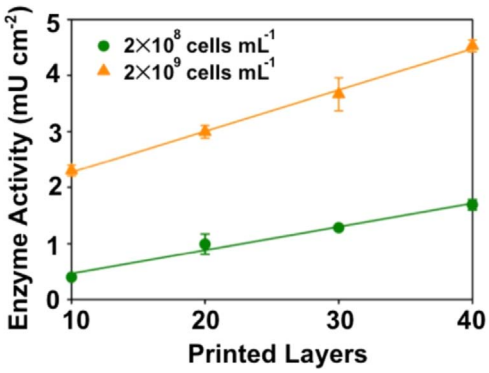

Fig. 3. Enzymatic activity of biocatalytic membranes (BCMs) evaluated as a function of the number of printed layers. The enzymatic activities of biocatalytic membranes prepared with an ink containing 2×10^8 cells mL^{-1} and an ink containing 2×10^9 cells mL^{-1} were quantified by measuring the oxidation of ABTS in batch reactions containing 0.2 cm^2 of BCMs. The curves were fitted by linear regression.

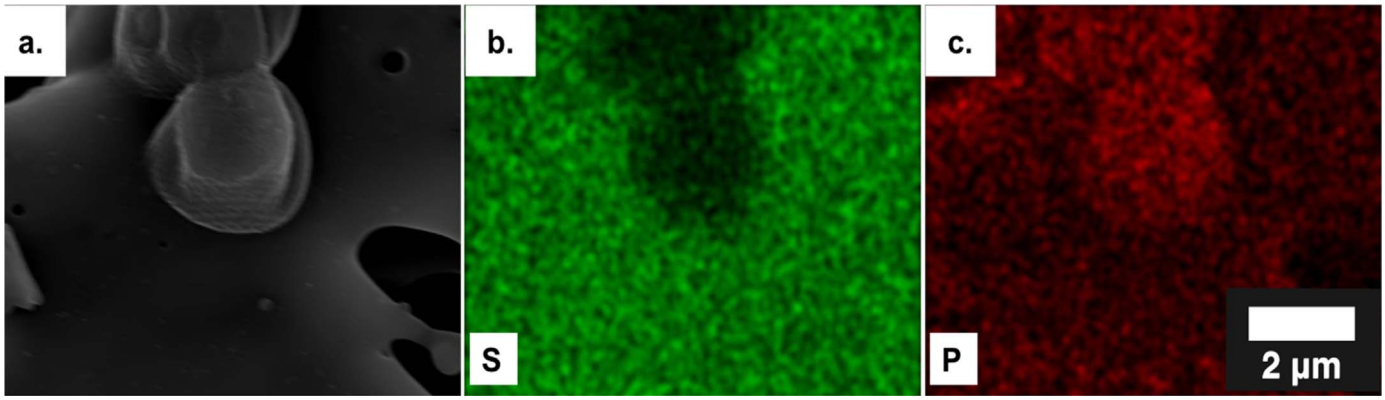

Fig. 2. Characterization of BCM morphology and elemental mapping. (a) A SEM micrograph of a yeast cell fixed to the surface of a biocatalytic membrane. Panels (b) and (c) show the corresponding energy-dispersive X-ray spectroscopy (EDX) elemental maps of the biocatalytic membrane for regions rich in sulfur, which appear green, and for regions rich in phosphate, which appear red. Yeast cells were fixed to the BCMs using the vapor above a 25% (by volume) glutaraldehyde solution and dehydrated using serial alcohol solutions prior to SEM and EDX analysis. (For interpretation of the references to color in this figure legend, the reader is referred to the web version of this article.)

Table 3
Membranes used in this study. The extent of redox mediator 2,2-azinobis-3-ethylbenzothiazoline-6-sulfonate (ABTS) oxidation mediated by laccase was indicated by the color change to green. All samples, except the parent membrane, were prepared using 30 overprints of the respective composite ink.

Membranes	Cell concentration (cells mL^{-1})	Enzyme activity of composite ink (U mL^{-1})	Crosslinking	Enzyme activity of composite membrane (mU cm^{-2})
Membrane [60]	N.A.	N.A.	N.A.	N.A.
BCM-0.2	2×10^8	0.2	No	2.23
BCM-0.2-X	2×10^8	0.2	Yes	1.28
BCM-2.0	2×10^9	2	No	6.31
BCM-2.0-X	2×10^9	2	Yes	3.71
EFM-0.2	N.A.	0.2	No	2.01
EFM-0.2-X	N.A.	0.2	Yes	BDL
EFM-2.0	N.A.	2	No	3.51
EFM-2.0-X	N.A.	2	Yes	1.41
M-0.0-X (control)	2×10^9	N.A.	Yes	N.A.

*BDL, below detection limit.

3.3. Functionality of BCMs

Enzyme functionalized membranes (EFMs) prepared using free laccase in the formulation of the composite inks were fabricated in order to compare the BCMs to a more conventional formulation. Virgin membranes and membranes prepared using yeast cells that do not express laccase were prepared as controls. The naming convention for membrane samples used in this set of experiments is summarized in Table 3. The number represents the initial enzymatic activity of the composite ink and the presence of an X indicates the sample had been crosslinked. After preparation, the activity of the samples was quantified using the oxidation of ABTS. The virgin membranes and membrane prepared with control cells did not exhibit ABTS oxidation. In comparison, the oxidation of ABTS was observed to varying degrees for the membranes functionalized with laccase. For crosslinked samples, the BCMs exhibited significant ABTS oxidation at 1 h, while EFMs did not. The lower enzyme activity of the crosslinked EFMs compared to BCMs might be attributed to the sensitivity of the free enzyme to the crosslinking treatment or mass transfer limitations for free enzymes sequestered within the crosslinked PVA. While further optimization of the EFM samples may result in higher activities, the current results demonstrate that SDL cells, which are easier to produce, can result in BCMs with competitive activity.

We hypothesized that the SDL cells were still viable after immobilization and capable of amplifying once incubated in a growth medium. This hypothesis was supported by the Live/Dead Yeast Viability assay performed in order to obtain the fluorescent micrograph shown in Fig. 1**a**. The high number of green cells indicated that the yeast cells remain viable. We next confirmed the viability of cells by an alternative approach of culturing the same BCM in yeast culturing medium. Two 1 cm^2 BCM-2.0-X samples were incubated at 30 °C and stirred at 250 rpm; one sample in 10 mL SC-trp medium containing 20 g L^{-1} glucose and the other in DI water. The cell growth (OD_{600}) was tracked over a 72 h period (Table S2). In this time, amplified cells were not detected in the DI water, suggesting no cell growth, but were detected in the synthetic growth medium. SDL cells that had been immobilized grew at a slower rate (0.13 h^{-1}) than suspended cells (0.22 h^{-1}) [21], and experienced a longer lag phase. However, the results suggest that the immobilized biocatalytic cells remain viable and multiply after deposition and crosslinking. Due to this convenient and efficient regeneration of immobilized cells, we envisioned that the enzyme activity of used BCMs could be renewed by immobilizing the amplified cells, but the properties of the regenerated BCMs including biocatalytic activity and permeability need to be carefully characterized in future studies.

3.4. Reusability and storage stability of the BCMs

A primary motivation for immobilization of the SDL yeast cells on microporous substrates was to facilitate recycling and reuse of the cells. The ability to recover and reuse BCMs was examined by quantifying the laccase activity in repeated ABTS oxidation reactions. Specifically, a BCM-0.2-X sample was submerged in an aqueous solution containing 0.7 mM ABTS buffered to pH 5 and the enzymatic activity was quantified for a period of 90 min. After 90 min, the BCM-0.2-X sample was extracted with tweezers, washed with acetate buffer solution, and then reused for another reaction cycle. The ability to reuse the suspended SDL cells was evaluated in parallel under the same conditions. Between reactions, the suspended cells were harvested by centrifugation and washed with acetate buffer solution before being reused. The results of these experiments are summarized in Fig. 4**a** where the relative activity

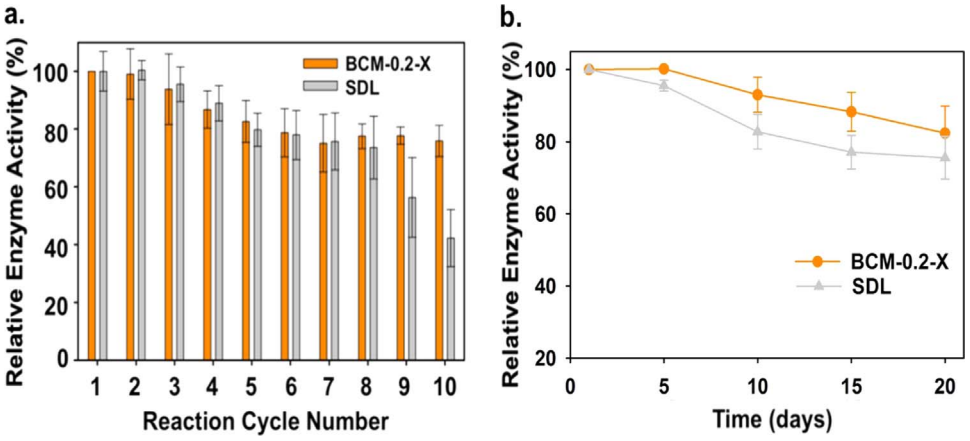

Fig. 4. Evaluation and comparison of reusability and storage stability of biocatalytic membranes (BCM-0.2-X) and suspended yeast cells with surface displayed laccase (SDL). (a) Reusability, indicating the ability to recover and reuse the BCM-0.2-X and the SDL cells, was evaluated in repeated ABTS oxidation reactions. The relative enzyme activity was obtained by taking the ratio of the enzyme activity at a given cycle to the initial enzyme activity at cycle 1. (b) The storage stability of the BCM-0.2-X and SDL cells was assessed over a period of 20 days with the samples being stored at room temperature. The relative enzyme activity was obtained by taking the ratio of the enzyme activity at a given time to the initial enzyme activity at day 0. ABTS oxidation was used to quantify enzyme activity. All the results are the means of triplicate experiments; error bars indicating standard deviations are not visible when smaller than the symbol size.

is plotted versus cycle number. The BCM-0.2-X underwent a slower recycle-induced loss of activity when compared to the suspended SDL cells. The two platforms follow the same trend until the eighth iteration of recycling (*t*-test, p = 0.97) after which a substantial loss in activity was noticed for the suspended cells (*t*-test, p = 0.05). By the end of the tenth cycle, the BCM-0.2-X retained 76% of its original activity while the suspended cells exhibited only 42% of their initial activity. The BCM-0.2-X was removed from the solution at the end of the tenth cycle and the liquid solution from reaction cycles 1–10 were centrifuged to collect any SDL cells that had become dislodged from the BCM. An enzyme assay on the SDL cells demonstrated an enzyme activity equal to 3.53 ± 0.62% of the initial BCM activity, suggesting that cell loss was not a major cause of the decrease in the activity of BCMs during reuse. Instead, reduction of enzyme activity of the SDL on the BCM was likely to be the main reason. The more rapid loss of activity observed in the suspended SDL system might be caused by damage to the cells that accumulated during centrifugation [61]. The results suggested that the BCMs with embedded SDL cells have a higher reusability than that of freely suspended SDL cells.

The stability of the BCMs during storage is another factor that affects their viability. Therefore, enzymatic activity was assessed intermittently while the BCM-0.2-X and suspended cells were stored exposed to the atmosphere at room temperature. ABTS enzyme assays were conducted every 5 days and relative enzyme activity was used to compare the two platforms (Fig. 4**b**). The results of these experiments demonstrated that the activity of the BCM-0.2-X declined gradually over the 20-day period in a similar pattern to the SDL. In our previous study [21], surface displayed laccase was found to improve the enzyme stability compared to free laccase. The SDL retained over 90% of the initial enzyme activity after 20 days storage at room temperature, while in contrast, activity of free laccase declined to 64% of its initial activity. In the current study, this beneficial feature of suspended SDL cells was maintained even after immobilization (*t*-test, p = 0.28), indicating the viability of cells after inkjet printing and crosslinking to a solid matrix. The results suggested that immobilizing SDL cells onto membrane substrates by inkjet printing is a promising approach to enhance reusability of the biocatalyst while retaining the stability.

3.5. Micropollutant BPA removal and degradation by BCMs

Membrane-based enzyme systems have been reported to be effective in the removal of persistent micropollutants [62,63]. Bisphenol A (BPA) is a notorious endocrine disrupting compound that is commonly leached from plastic products [64–66]. Due to its persistence and poor removal in conventional wastewater treatment processes, BPA has been widely detected in wastewater effluents and natural environments at trace levels (370 μg L^{-1} to 0.0006 ng L^{-1}) [67]. Our previous study demonstrated that the SDL cells were effective in treating BPA [21]. Here, batch experiments using BPA as a proof-of-concept substrate were conducted to assess the effectiveness of BCMs in removing and degrading persistent micropollutants. Reaction vials were filled with an aqueous solution at pH = 5 that contained 1 μM BPA, with or without the addition of the redox mediator ABTS (1 μM). Redox mediators, of which ATBS is a commonly used example [68], are molecules that can enhance the reactivity of enzymes by acting as electron shuttles between the active site of an enzyme and target compound [69,70]. The overall removal efficiency, which is defined as the percent decrease in BPA concentration at an arbitrary time relative to the BPA concentration at the initial time, t = 0, is shown in Fig. 5**a**. After 9 h, 53% and 74% of the BPA present in solution was removed by BCM-2.0-X without and with the addition of ABTS, respectively. In comparison, the suspended SDL cells without and with the addition of ATBS removed only 9% and 26% of the BPA, respectively.

The BPA concentration decreased substantially, by ~ 44%, within 30 min of adding the BCM-2.0-X to the reaction vials. A similar reduction was observed for vials containing a membrane functionalized with control cells that displayed no laccase, while around 60% of the BPA was removed from solution by a bare membrane (Fig. S3). Despite the rapid, initial drop in concentration for these two controls, the BPA concentrations did not decrease significantly in the subsequent 9 h. In comparison, BPA was continuously removed by BCMs functionalized with SDL yeast cells. These results suggest a rapid adsorption of BPA by the cell and membrane surfaces followed by the enzymatic degradation of BPA by the SDL cells. Therefore, it seemed reasonable to assume that BPA adsorption saturated rapidly, and that the subsequent BPA removal after the first sampling point could be attributed to enzymatic degradation. Based on this assumption, the following equation was used to determine the BPA degradation efficiency due to laccase activity,

$$\text{degradation efficiency}\,(\%) = \frac{C_1 - C_t}{C_1} \times 100\% \quad (1)$$

where C_t is the BPA concentration at time *t*, and C_1 is the BPA concentration at the first sampling point, that is, at t = 30 min. The degradation efficiency of BPA by suspended SDL was obtained using the same procedure. A comparison of the degradation efficiency is presented in Fig. 5**b**. Notably, the degradation of BPA by the BCM-2.0-X was higher than that of the suspended SDL cells (*t*-test, p = 0.07). The degradation efficiency of BPA by BCM-2.0-X at 9 h was 20% and the degradation efficiency increased to 54% through the addition of ABTS. In comparison, only 3% and 23% of the BPA was degraded by suspended SDL cells with or without the addition of ABTS, respectively.

The results suggested that adsorption of BPA to the BCM may stimulate its degradation. Adsorption is a common phenomenon in membrane processes aiming at the removal of micropollutants [71,72], especially for hydrophobic compounds such as BPA, which has a $\log K_{ow}$ as high as 3.32 where K_{ow} denotes octanol-water partition coefficient [73]. Due to the ubiquitous nature of this phenomenon, a dedicated study focused on elucidating the adsorption characteristics of BPA on polysulfone membranes concluded that the adsorption was driven by the hydrophobicity of the BPA as well as the ability of hydrogen bonds to form between the hydroxyl group of BPA and polysulfone [74]. The adsorption of BPA could concentrate the micropollutant on the

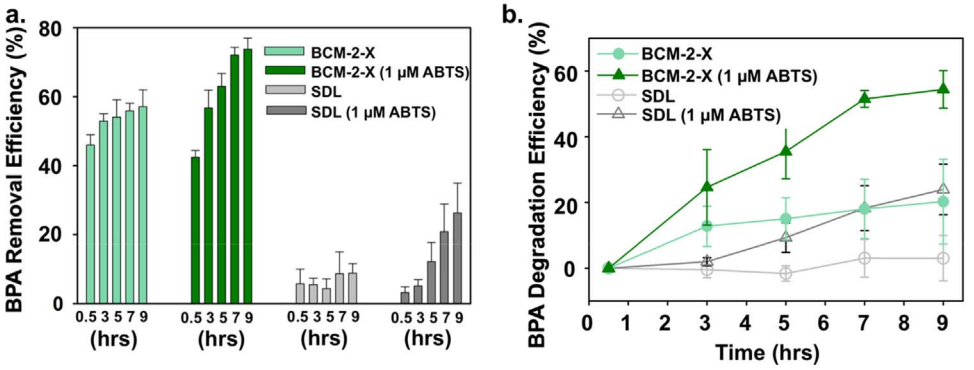

Fig. 5. Biocatalytic membranes effectively removed and degraded bisphenol A. The removal and degradation of BPA by surface displayed laccase biocatalytic cells is shown for comparison. **(a)** Overall BPA removal efficiency by the BCM-2.0-X or SDL cells under conditions without or with the addition of the redox mediator ABTS (1 μM). **(b)** Degradation efficiencies of BPA by the BCM-2.0-X or SDL cells under conditions with or without the addition of the redox mediator ABTS (1 μM). The initial BPA concentration was 1 μM. The initial enzyme activity for all the reactions was set as 0.4 mU mL^{-1} of the micropollutant-containing solution. Results are the means of triplicate experiments; error bars indicating standard deviations are not visible when smaller than the symbol size.

membrane matrix and increase the probability of interactions between the active sites of the enzyme and BPA molecules. The adsorption of contaminants on solid substrates such as membranes has been widely reported [75,76], but the ability of adsorption to enhanced biocatalytic activity of enzymatically-active materials has been rarely reported. One previous study reported the use of laccase-carrying membranes for treatment of polycyclic aromatic hydrocarbons (PAHs) in soils [63], the removal efficiency of PAHs by the laccase-functionalized membranes reached 70% while the removal efficiency by free laccase was only 30%, which suggested a synergistic effect between adsorption onto the membrane and degradation by the enzyme enhanced the removal of PAHs.

3.6. Micropollutant APAP degradation by BCMs

To further assess the potential of the BCMs for micropollutant degradation beyond BPA, the medication APAP was examined as another model substrate. APAP is a widely used and abused analgesic and antipyretic drug [77]. It cannot be effectively removed by conventional wastewater treatment processes and is among the most frequently detected pharmaceutical and personal care products in natural and drinking waters (1000 μg L^{-1} to 0.01 ng L^{-1}) [78,79]. Moreover, APAP is much more hydrophilic than BPA; the $\log K_{ow}$ for APAP is 0.46 [2] while the $\log K_{ow}$ for BPA is 3.32 [73]. Therefore, using APAP as a substrate provides a distinct scenario to evaluate the biocatalytic ability of the BCMs with little adsorption of the target contaminant. Batch experiments were conducted in acetic acid buffer (pH = 5) containing 1 μM APAP (Fig. 6). Adsorption of APAP to the BCMs was found to be insignificant. Therefore, the removal of APAP was due to enzymatic degradation. The degradation efficiency of APAP by the BCM-2.0-X and SDL with the addition of ABTS reached 94.4% and 99.8%, respectively, after 12 h of incubation. Considering the same initial enzyme activity for the BCMs and SDLs (0.4 U/mL) used in the experiment, the similar degradation efficiency of APAP by the two platforms indicated that there were no limiting factors (e.g., mass transfer limitation) for APAP degradation by the BCMs relative to the suspended SDLs. Regardless of platform, it was noted that the degradation of APAP was only 10% without the addition of ABTS, indicating that the access of the APAP molecule to the active laccase enzyme sites on cell surface might be a limiting factor for its degradation.

The results indicated that adsorption of micropollutants to the BCMs could also affect the degradation mechanism of the micropollutants. Specifically, in this study the BCMs and SDLs degraded APAP, which has a lower K_{ow} value and exhibited little adsorption to the membrane, at the same rate. Conversely, the BCMs degraded BPA, which has a higher K_{ow} value and adsorbed to the membrane, more rapidly than the SDLs did. This suggests that in the fabrication of BCMs it might be possible to pick substrates that foster micropollutant-BCM interactions in order to enhance activity and degradation rates.

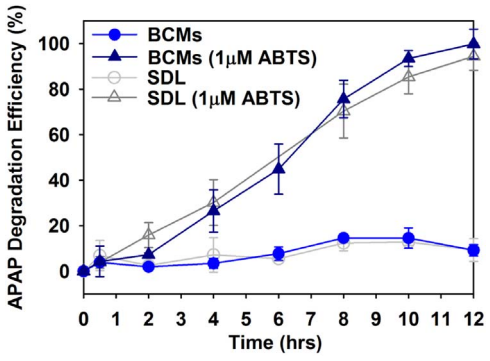

Fig. 6. Biocatalytic membranes effectively degraded acetaminophen. The degradation of APAP by surface displayed laccase biocatalytic cells is shown for comparison. Degradation efficiencies of APAP by the BCM-2.0-X or SDL cells under conditions with or without the addition of the redox mediator ABTS (1 μM). The initial APAP concentration was 1 μM. The initial enzyme activity for all the reactions was set as 0.4 mU mL^{-1} of the micropollutant-containing solution. Results are the means of triplicate experiments; error bars indicating standard deviations are not visible when smaller than the symbol size.

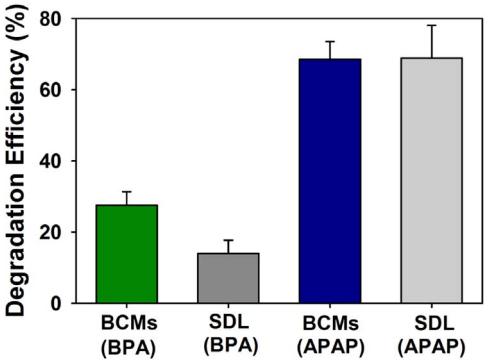

Fig. 7. BCMs can degrade bisphenol A (BPA) and acetaminophen (APAP) amended in filtered secondary wastewater effluent. Degradation efficiencies of BPA after 9 h or APAP after 12 h by the BCM-2.0-X or SDL cells were shown under conditions with the addition of the redox mediator ABTS (1 μM). The initial BPA or APAP concentration was 1 μM. The initial enzyme activity for all the reactions was set as 0.4 mU mL^{-1} of the micropollutant-containing solution. Results are the means of triplicate experiments; error bars indicating standard deviations are not visible when smaller than the symbol size.

Finally, we performed batch experiments with filtered secondary wastewater effluent. BPA was amended to obtain an initial concentration of 1 μM. The degradation efficiency of BPA by the BCMs with addition of 1 μM ABTS reached 28 ± 4% after 9 h of reaction (Fig. 7), while the incubation with SDL cells had only 14 ± 4% BPA degradation under the same experimental conditions. Similar results were observed for degradation of 1 μM APAP amended in filtered secondary wastewater effluent by BCMs and SDL (Fig. 7). BCMs and SDL biocatalyst degraded 69 ± 5% and 69 ± 9% APAP in 12 h with the addition of 1 μM ABTS. Taken together, these results demonstrated that BCMs can effectively degrade a more hydrophilic contaminant, APAP, in both a buffer and under environmental relevant conditions upon the addition of a laccase mediator.

The hydraulic permeability of the BCMs was also considered in the design of the printing process. In this demonstration of the BCM platform, we wanted to ensure that the SDL cells could be affixed throughout the membrane substrate. Therefore, a microfiltration membrane with large micron-sized pores and a permeability of ~ 44,000 L m^{-2} h^{-1} bar^{-1} was chosen as the substrate. As the number of printed layers increased and a greater number of cells were deposited onto the membrane substrate, the permeability decreased (Fig. S4). However, the value of the permeability for the membranes used in the micropollutant degradation experiments was ~ 10,000 L m^{-2} h^{-1} bar^{-1}. Based on the biocatalytic activity of the BCMs, this membrane would not work well in the flow-through configuration we ultimately envision for the platform because the characteristic time for flow is much shorter than the characteristic time for contaminant degradation. This provides another criterion for the further development of the BCM platform that has been demonstrated here. Specifically, the times for reaction and flow should be on the same order of magnitude for optimal performance. This goal can be accomplished with further optimization of the SDL biocatalyst to achieve higher enzyme activity or by selecting a less permeable membrane (e.g., a nanofiltration membrane or an ultrafiltration membrane) as the parent substrate. The flexibility of the BCM fabrication process that we demonstrated here allows for these new higher performance BCMs to be produced in a straightforward manner and provides exciting opportunities for further optimizing this reactive membrane platform.

4. Conclusions

In this study, yeast cells that expressed surface-displayed laccase were deposited onto microporous substrates using inkjet printing.

Notably, enzymatically-active membranes that effectively treated aqueous solutions containing bisphenol A and acetaminophen resulted. Due to the wide substrate range of fungal laccase, this platform is anticipated to effectively treat other persistent organic micropollutants. The BCMs were resilient and could be recycled and reused in multiple treatment cycles, while the immobilized cells could be regenerated by simple cultivation. We envision the use of BCMs as a promising advanced treatment alternative in water reclamation and reuse scenarios. The technology could be either operated alone (*e.g.* advanced treatment of tertiary effluent) or in combination with current advanced treatment technologies (e.g. treatment of reverse osmosis concentrate, a challenging waste stream in inland desalination and reuse [80,81]). While our study suggested the high performance of BCMs in batch experiments, the ability of BCMs to degrade contaminants during continuous filtration processes is an important direction of future study. Such studies would help to identify the range of applicability of BCMs and provide knowledge to focus further development of the platform. In addition, by modifying the biocatalytic cells to express different enzymes or implementing other membrane substrates with varied permselectivities, BCMs with functionality tailored for targeted applications could be created using the modular nature of the inkjet printing process. The resulting BCMs could be applied to address challenges relevant to other facets of the food-water-energy nexus.

Acknowledgements

This work was supported in part by the National Science Foundation (Award no. 1653679), U.S. Department of Energy, Basic Energy Sciences, Division of Materials Sciences and Engineering, under Contract DE-FG02-05ER46222. Y.C. thankfully acknowledges support from the ND Center for Environmental Science and Technology Predoctoral Fellowship Program. P.G. thankfully acknowledges support from the ND Energy Postdoctoral Fellowship Program and M.J.S. gratefully acknowledges support from the CEST/Bayer Pre-Doctoral Research Fellowship at the University of Notre Dame. We thank the Notre Dame Integrated Imaging Facility (NDIIF) and the Center for Environmental Science and Technology (CEST) at Notre Dame; portions of this research were performed with instruments at these facilities.

Appendix A. Supporting information

Supplementary data associated with this article can be found in the online version at http://dx.doi.org/10.1016/j.memsci.2017.12.045.

References

[1] X. Yang, R.C. Flowers, H.S. Weinberg, P.C. Singer, Occurrence and removal of pharmaceuticals and personal care products (PPCPs) in an advanced wastewater reclamation plant, Water Res. 45 (2011) 5218–5228.
[2] B. Petrie, R. Barden, B. Kasprzyk-Hordern, A review on emerging contaminants in wastewaters and the environment: current knowledge, understudied areas and recommendations for future monitoring, Water Res. 72 (2015) 3–27.
[3] M. Poliakoff, J.M. Fitzpatrick, T.R. Farren, P.T. Anastas, Green chemistry: science and politics of change, Science 297 (2002) 807–810.
[4] Fv Rantwijk, Biocatalysis for sustainable organic Synthesis, Aust. J. Chem. 57 (2004) 281–289.
[5] D.H. Zhang, L.X. Yuwen, L.J. Peng, Parameters affecting the performance of immobilized, Enzym. J. Chem. (2013).
[6] S. Yang, F.I. Hai, L.D. Nghiem, W.E. Price, F. Roddick, M.T. Moreira, S.F. Magram, Understanding the factors controlling the removal of trace organic contaminants by white-rot fungi and their lignin modifying enzymes: a critical review, Bioresour. Technol. 141 (2013) 97–108.
[7] Y.J. Kim, J.A. Nicell, Impact of reaction conditions on the laccase-catalyzed conversion of bisphenol A, Bioresour. Technol. 97 (2006) 1431–1442.
[8] T. Saito, K. Kato, Y. Yokogawa, M. Nishida, N. Yamashita, Detoxification of bisphenol A and nonylphenol by purified extracellular laccase from a fungus isolated from soil, J. Biosci. Bioeng. 98 (2004) 64–66.
[9] Y. Tamagawa, H. Hirai, S. Kawai, T. Nishida, Removal of estrogenic activity of endocrine-disrupting genistein by ligninolytic enzymes from white rot fungi, FEMS Microbiol. Lett. 244 (2005) 93–98.
[10] M. Auriol, Y. Filali-Meknassi, C.D. Adams, R.D. Tyagi, T.-N. Noguerol, B. Pina, Removal of estrogenic activity of natural and synthetic hormones from a municipal wastewater: efficiency of horseradish peroxidase and laccase from *Trametes versicolor*, Chemosphere 70 (2008) 445–452.
[11] A.C. Bastos, N. Magan, *Trametes versicolor*: potential for atrazine bioremediation in calcareous clay soil, under low water availability conditions, Int. Biodeterior. Biodegrad. 63 (2009) 389–394.
[12] J. Margot, P.-J. Copin, U. von Gunten, D.A. Barry, C. Holliger, Sulfamethoxazole and isoproturon degradation and detoxification by a laccase-mediator system: influence of treatment conditions and mechanistic aspects, Biochem. Eng. J. 103 (2015) 47–59.
[13] J.M. Hutchison, S.K. Poust, M. Kumar, D.M. Cropek, I.E. MacAllister, C.M. Arnett, J.L. Zilles, Perchlorate reduction using free and encapsulated *Azospira oryzae* enzymes, Environ. Sci. Technol. 47 (2013) 9934–9941.
[14] J.M. Hutchison, J.L. Zilles, Biocatalytic perchlorate reduction: kinetics and effects of groundwater characteristics, Environ. Sci.: Water Res. Technol. 1 (2015) 913–921.
[15] C.C. de Carvalho, Enzymatic and whole cell catalysis: finding new strategies for old processes, Biotechnol. Adv. 29 (2011) 75–83.
[16] A. Schmid, J. Dordick, B. Hauer, A. Kiener, M. Wubbolts, B. Witholt, Industrial biocatalysis today and tomorrow, Nature 409 (2001) 258–268.
[17] Y. Ni, R.R. Chen, Accelerating whole-cell biocatalysis by reducing outer membrane permeability barrier, Biotechnol. Bioeng. 87 (2004) 804–811.
[18] L. Cao, Carrier-bound Immobilized Enzymes: Principles, Applications and Design, Wiley-VCH, Weinheim, 2005.
[19] K. Kuroda, M. Ueda, Arming technology in yeast-novel strategy for whole-cell biocatalyst and protein engineering, Biomolecules 3 (2013) 632–650.
[20] S.Y. Lee, J.H. Choi, Z. Xu, Microbial cell-surface display, Trends Biotechnol. 21 (2003) 45–52.
[21] Y. Chen, B. Stemple, M. Kumar, N. Wei, Cell surface display fungal laccase as a renewable biocatalyst for degradation of persistent micropollutants bisphenol A and sulfamethoxazole, Environ. Sci. Technol. 50 (2016) 8799–8808.
[22] C.S. Evans, Laccase activity in lignin degradation by Coriolus versicolor in vivo and in vitro studies, FEMS Microbiol. Lett. 27 (1985) 339–343.
[23] S.R. Couto, J.L.T. Herrera, Industrial and biotechnological applications of laccases: a review, Biotechnol. Adv. 24 (2006) 500–513.
[24] C.D. Scott, Immobilized cells: a review of recent literature, Enzym. Microb. Technol. 9 (1987) 66–72.
[25] T. Johannes, M.R. Simurdiak, H. Zhao, Biocatalysis, in: Encyclopedia of Chemical Processing, 2006, pp. 101–110.
[26] A.M. Klibanov, Immobilized enzymes and cells as practical catalysts, Science 219 (1983) 722–727.
[27] I. Stolarzewicz, E. Białecka-Florjańczyk, E. Majewska, J. Krzyczkowska, Immobilization of yeast on polymeric supports, Chem. Biochem. Eng. Q. 25 (2011) 135–144.
[28] V.C. Gekas, Artificial membranes as carriers for the immobilization of biocatalysts, Enzym. Microb. Technol. 8 (1986) 450–460.
[29] D.S. Inloes, D.P. Taylor, S.N. Cohen, A.S. Michaels, C.R. Robertson, Ethanol production by Saccharomyces cerevisiae immobilized in hollow-fiber membrane bioreactors, Appl. Environ. Microbiol. 46 (1983) 264–278.
[30] K.H. Kyung, P. Gerhardt, Continuous production of ethanol by yeast “immobilized” in a membrane-contained fermentor, Biotechnol. Bioeng. 26 (1984) 252–256.
[31] J. Luo, A.S. Meyer, R.V. Mateiu, D. Kalyani, M. Pinelo, Functionalization of a membrane sublayer using reverse filtration of enzymes and dopamine coating, ACS Appl. Mater. Interfaces 6 (2014) 22894–22904.
[32] S.C.S. Martins, C.M. Martins, L.M.C.G. Fiúza, S.T. Santaella, Immobilization of microbial cells: a promising tool for treatment of toxic pollutants in industrial wastewater, Afr. J. Biotechnol. 12 (2013).
[33] P. Calvert, Inkjet printing for materials and devices, Chem. Mater. 13 (2001) 3299–3305.
[34] C.M. Andres, N.A. Kotov, Inkjet deposition of layer-by-layer assembled films, J. Am. Chem. Soc. 132 (2010) 14496–14502.
[35] P. Gao, A. Hunter, S. Benavides, M.J. Summe, F. Gao, W.A. Phillip, Template synthesis of nanostructured polymeric membranes by inkjet printing, ACS Appl. Mater. Interfaces 8 (2016) 3386–3395.
[36] P. Gao, A. Hunter, M.J. Summe, W.A. Phillip, A. Method, for the efficient fabrication of multifunctional mosaic membranes by inkjet printing, ACS Appl. Mater. Interfaces 8 (2016) 19772–19779.
[37] L. Gonzalez-Macia, A. Morrin, M.R. Smyth, A.J. Killard, Advanced printing and deposition methodologies for the fabrication of biosensors and biodevices, Analyst 135 (2010) 845–867.
[38] A.V. Parry, A.J. Straub, E.M. Villar-Alvarez, T. Phuengphol, J.E. Nicoll, L.M. Jordan, K.L. Moore, P. Taboada, S.G. Yeates, S. Edmondson, Submicron patterning of polymer Brushes: an unexpected discovery from inkjet printing of polyelectrolyte macroinitiators, J. Am. Chem. Soc. 138 (2016) 9009–9012.
[39] Y. Wang, L. Zhang, J. Wu, M.N. Hedhili, P. Wang, A facile strategy for the fabrication of a bioinspired hydrophilic–superhydrophobic patterned surface for highly efficient fog-harvesting, J. Mater. Chem. A 3 (2015) 18963–18969.
[40] A.S. Gladman, E.A. Matsumoto, R.G. Nuzzo, L. Mahadevan, J.A. Lewis, Biomimetic 4D printing, Nat. Mater. (2016).
[41] E. Cheng, H. Yu, A. Ahmadi, K.C. Cheung, Investigation of the hydrodynamic response of cells in drop on demand piezoelectric inkjet nozzles, Biofabrication 8 (2016) 015008.
[42] R.E. Saunders, B. Derby, Inkjet printing biomaterials for tissue engineering: bioprinting, Int. Mater. Rev. 59 (2014) 430–448.
[43] B.J. de Gans, P.C. Duineveld, U.S. Schubert, Inkjet printing of polymers: state of the art and future developments, Adv. Mater. 16 (2004) 203–213.

[44] E. Tekin, P.J. Smith, U.S. Schubert, Inkjet printing as a deposition and patterning tool for polymers and inorganic particles, Soft Matter 4 (2008) 703–713.
[45] B. Derby, Inkjet printing of functional and structural materials: fluid property requirements, feature stability, and resolution, Annu. Rev. Mater. Res. 40 (2010) 395–414.
[46] H. Gudupati, M. Dey, I. Ozbolat, A comprehensive review on droplet-based bioprinting: Past, Present and Future, Biomaterials 102 (2016) 20–42.
[47] T. Xu, J. Jin, C. Gregory, J.J. Hickman, T. Boland, Inkjet printing of viable mammalian cells, Biomaterials 26 (2005) 93–99.
[48] J. Merrin, S. Leibler, J.S. Chuang, Printing multistrain bacterial patterns with a piezoelectric inkjet printer, PLoS One 2 (2007) e663.
[49] I. Drachuk, R. Suntivich, R. Calabrese, S. Harbaugh, N. Kelley-Loughnane, D.L. Kaplan, M. Stone, V.V. Tsukruk, Printed dual cell arrays for multiplexed sensing, ACS Biomater. Sci. Eng. 1 (2015) 287–294.
[50] N. Komuro, S. Takaki, K. Suzuki, D. Citterio, Inkjet printed (bio) chemical sensing devices, Anal. Bioanal. Chem. 405 (2013) 5785–5805.
[51] R.D. Gietz, R.H. Schiestl, High-efficiency yeast transformation using the LiAc/SS carrier DNA/PEG method, Nat. Protoc. 2 (2007) 31–34.
[52] G. Chao, W.L. Lau, B.J. Hackel, S.L. Sazinsky, S.M. Lippow, K.D. Wittrup, Isolating and engineering human antibodies using yeast surface display, Nat. Protoc. 1 (2006) 755–768.
[53] S. Qu, T. Dilenschneider, W.A. Phillip, Preparation of chemically-tailored copolymer membranes with tunable ion transport properties, ACS Appl. Mater. Interfaces 7 (2015) 19746–19754.
[54] J.D. Schiffman, M. Elimelech, Antibacterial activity of electrospun polymer mats with incorporated narrow diameter single-walled carbon nanotubes, ACS Appl. Mater. Interfaces 3 (2011) 462–468.
[55] G. Bleve, C. Lezzi, S. Spagnolo, P. Rampino, C. Perrotta, G. Mita, F. Grieco, Construction of a laccase chimerical gene: recombinant protein characterization and gene expression via yeast surface display, Appl. Biochem. Biotechnol. 172 (2014) 2916–2931.
[56] K. Koschorreck, S.M. Richter, A. Swierczek, U. Beifuss, R.D. Schmid, V.B. Urlacher, Comparative characterization of four laccases from Trametes versicolor concerning phenolic C–C coupling and oxidation of PAHs, Arch. Biochem. Biophys. 474 (2008) 213–219.
[57] C. Johannes, A. Majcherczyk, Laccase activity tests and laccase inhibitors, J. Biotechnol. 78 (2000) 193–199.
[58] W.E. Federation, A.P.H. Association, Standard Methods for the Examination of Water and Wastewater, American Public Health Association (APHA), Washington, DC, USA, 2005.
[59] G. Paradossi, F. Cavalieri, E. Chiessi, C. Spagnoli, M.K. Cowman, Poly (vinyl alcohol) as versatile biomaterial for potential biomedical applications, J. Mater. Sci.: Mater. Med. 14 (2003) 687–691.
[60] W.J. Wrasidlo, Asymmetric membranes, in, Google Patents, 1986.
[61] B.W. Peterson, P.K. Sharma, H.C. van der Mei, H.J. Busscher, Bacterial cell surface damage due to centrifugal compaction, Appl. Environ. Microbiol. 78 (2012) 120–125.
[62] J. Hou, G. Dong, Y. Ye, V. Chen, Enzymatic degradation of bisphenol-A with immobilized laccase on TiO 2 sol–gel coated PVDF membrane, J. Membr. Sci. 469 (2014) 19–30.
[63] Y. Dai, L. Yin, J. Niu, Laccase-carrying electrospun fibrous membranes for adsorption and degradation of PAHs in shoal soils, Environ. Sci. Technol. 45 (2011) 10611–10618.
[64] L.N. Vandenberg, R. Hauser, M. Marcus, N. Olea, W.V. Welshons, Human exposure to bisphenol A (BPA), Reprod. Toxicol. 24 (2007) 139–177.
[65] M. Murugananthan, S. Yoshihara, T. Rakuma, T. Shirakashi, Mineralization of bisphenol A (BPA) by anodic oxidation with boron-doped diamond (BDD) electrode, J. Hazard. Mater. 154 (2008) 213–220.
[66] C. Arboleda, H. Cabana, E. De Pril, J.P. Jones, G. Jiménez, A. Mejía, S.N. Agathos, M. Penninckx, Elimination of bisphenol A and triclosan using the enzymatic system of autochthonous Colombian forest fungi, ISRN Biotechnol. 2012 (2013).
[67] J. Corrales, L.A. Kristofco, W.B. Steele, B.S. Yates, C.S. Breed, E.S. Williams, B.W. Brooks, Global assessment of bisphenol A in the environment: review and analysis of its occurrence and bioaccumulation, Dose-Response 13 (2015).
[68] K.G. Arzola, M.C. Arevalo, M.A. Falcon, Catalytic efficiency of natural and synthetic compounds used as laccase-mediators in oxidising veratryl alcohol and a kraft lignin, estimated by electrochemical analysis, Electrochim. Acta 54 (2009) 2621–2629.
[69] S. Riva, Laccases: blue enzymes for green chemistry, Trends Biotechnol. 24 (2006) 219–226.
[70] O.V. Morozova, G.P. Shumakovich, S.V. Shleev, Y.I. Yaropolov, Laccase-mediator systems and their applications: a review, Appl. Biochem. Microbiol. 43 (2007) 523–535.
[71] A.M. Comerton, R.C. Andrews, D.M. Bagley, P. Yang, Membrane adsorption of endocrine disrupting compounds and pharmaceutically active compounds, J. Membr. Sci. 303 (2007) 267–277.
[72] A.I. Schäfer, I. Akanyeti, A.J. Semião, Micropollutant sorption to membrane polymers: a review of mechanisms for estrogens, Adv. Colloid Interface Sci. 164 (2011) 100–117.
[73] S. Vigneswaran, Waste Water Treatment Technologies - Volume I, EOLSS Publications, Oxford, United Kingdom, 2009.
[74] W. Su-Hua, D. Bing-zhi, H. Yu, Adsorption of bisphenol A by polysulphone membrane, Desalination 253 (2010) 22–29.
[75] R. Xu, C. Chi, F. Li, B. Zhang, Laccase–polyacrylonitrile nanofibrous membrane: highly immobilized, stable, reusable, and efficacious for 2, 4, 6-trichlorophenol removal, ACS Appl. Mater. Interfaces 5 (2013) 12554–12560.
[76] R. Xu, Q. Zhou, F. Li, B. Zhang, Laccase immobilization on chitosan/poly (vinyl alcohol) composite nanofibrous membranes for 2, 4-dichlorophenol removal, Chem. Eng. J. 222 (2013) 321–329.
[77] B. De Gusseme, L. Vanhaecke, W. Verstraete, N. Boon, Degradation of acetaminophen by Delftia tsuruhatensis and Pseudomonas aeruginosa in a membrane bioreactor, Water Res. 45 (2011) 1829–1837.
[78] M.D.G. de Luna, M.L. Veciana, C.-C. Su, M.-C. Lu, Acetaminophen degradation by electro-Fenton and photoelectro-Fenton using a double cathode electrochemical cell, J. Hazard. Mater. 217 (2012) 200–207.
[79] M.D.G. de Luna, M.L. Veciana, C.-C. Su, M.-C. Lu, Acetaminophen degradation by electro-Fenton and photoelectro-Fenton using a double cathode electrochemical cell, J. Hazard. Mater. 217 (2012) 200–207.
[80] S.H. Joo, B. Tansel, Novel technologies for reverse osmosis concentrate treatment: a review, J. Environ. Manag. 150 (2015) 322–335.
[81] P. Chelme-Ayala, D.W. Smith, M.G. El-Din, Membrane concentrate management options: a comprehensive critical review, Can. J. Civ. Eng. 36 (2009) 1107–1119.